




Biosorption of Nickel from Metal Finishing Effluent Using Lichen *Parmotrema tinctorum* Biomass

Zibia Kasturi Gratia · Raju Nandhakumar · Biswanath Mahanty  ·
Sevanan Murugan · Palanimuthu Muthusamy ·
Kanivebagilu Shankarnarayana Vinayak

Received: 16 August 2021 / Accepted: 8 November 2021 / Published online: 16 November 2021
© The Author(s), under exclusive licence to Springer Nature Switzerland AG 2021

Abstract Presence of heavy metals in industrial discharge warrants the adoption of efficient and cost-effective treatment technologies. In this work, lichen *Parmotrema tinctorum* biomass was utilized as biosorbent for removal of Ni (II) from metal finishing industry effluents. Optimal adsorption was observed at pH 7, stirring speed of 300 rpm, 120 min incubation from independent batch experiments. Adsorption isotherm at optimal conditions followed Langmuir model ($R^2 > 0.974$) with a maximum adsorption capacity of 33.92 mg g^{-1} . Adsorption kinetics could be described with pseudo-first-order model ($R^2 > 0.98$). Fourier transform infrared spectroscopy of pristine and metal loaded *P. tinctorum* biomass indicated electrostatics and ionic interaction in the adsorption process. Biosorbent treated water showed no inhibition against agriculturally important microorganisms like *Phosphobacter* sp. and *Azospirillum* sp.

in microbial toxicity assay. Similarly, biosorbent treated water offered better germination and growth for *Vigna radiata* than the untreated water in greenhouse phytotoxicity assessment. Though the result suggests detoxification of industrial effluents following *P. tinctorum* biosorption, reusability of treated wastewater in agricultural practice warrants multi-tiered ecotoxicity assessment, and long-term environmental impact analysis.

Keywords Biosorption · Isotherm · Kinetics · Nickel · *Parmotrema tinctorum* · Phytotoxicity

1 Introduction

Disposal of heavy-metal-laden industrial wastewater into the soil–water continuum appears to be a global

Z. K. Gratia · B. Mahanty (✉) · S. Murugan (✉)
Department of Biotechnology, Karunya Institute
of Technology and Sciences, Karunya Nagar, Coimbatore,
Tamil Nadu 641114, India
e-mail: bmahanty@karunya.edu

S. Murugan
e-mail: murugan@karunya.edu

Z. K. Gratia
e-mail: zibiakasturigratia@americancollege.edu.in

Z. K. Gratia
Department of Industrial Biotechnology, The American
College, Madurai, Tamil Nadu 625002, India

R. Nandhakumar
Department of Applied Chemistry, Karunya Institute
of Technology and Sciences, Karunya Nagar, Coimbatore,
Tamil Nadu 641114, India
e-mail: nandhakumar@karunya.edu

P. Muthusamy
Department of Food Technology, Excel Engineering
College, Komarapalayam, Tamil Nadu 637303, India
e-mail: pmuthusamy.eec@excelcolleges.com

K. S. Vinayak
Department of Botany, Sri Venkataramana Swamy
College, Vidyagiri, Bantwal, Karnataka 574211, India
e-mail: ks.vinayaka@gmail.com

environmental concern (V. Kumar et al., 2019). Wastewater if released untreated, the non-biodegradable, persistent heavy metals can bioaccumulate in the food chain and can be a threat to the ecosystem (Gitet et al., 2016; S. Gupta et al., 2010). Nickel, one of the key heavy metals, is widely used in mining, electroplating, and metal processing industries where concentration in electroplating effluents could be as high as 1000 mg l^{-1} (Duong et al., 2019; Min et al., 2019). Due to increased mobility in acidic soils, nickel can seep into the groundwater (Mamindy-Pajany et al., 2013).

As a common source of heavy metal poisoning, nickel has been associated with carcinogenic, teratogenic, and mutagenic potential even at concentrations of about $1.0\text{--}10 \text{ mg l}^{-1}$ (Martinez et al., 2019; Peters et al., 2016). Long-term exposure to nickel can cause cancer and lung fibrosis, as well as dermatitis (Buxton et al., 2019; Gad, 2014). The permissible limit of nickel in drinking water, according to the U.S. Environmental Protection Agency (EPA), is 0.02 mg l^{-1} (USEPA, 1986). Electroplating industries in India are mandated to keep a nickel concentration below 3 mg l^{-1} in the effluent (CPCB, 2012).

Several treatment modalities have been suggested for the removal of nickel from industrial effluents using conventional physico-chemical processes such as precipitation (Mubarok & Lieberto, 2013), ion exchange, electrochemical process, electro dialysis (C. Wang et al., 2020), and/or membrane distillation (Duong et al., 2019) processes are commonly applied for the treatment of industrial effluents. However, due to technical or economical constraints, the application of such processes is somehow restricted. The need for simple, economical, and effective separation technologies for removing heavy metals from wastewater streams is rational.

Due to metal binding capacities of varied biological material, utilization of biomass resources for removal of toxic metals from wastewater has been promising (Jianlong Wang & Chen, 2009). Inactive and dead biomass can remove heavy metals from dilute solutions based on their intrinsic property to bind and accumulate these pollutants either through ion exchange, precipitation, or sorption by physical forces (Javanbakht et al., 2014). Following metal biosorption, acute toxicity of effluent wastewater can significantly be reduced as often been measured in

bacterial or plant-based bioassay systems (Hemachandra & Pathiratne, 2015; Khan et al., 2019), such as suitability in seed germination which can vouch for reuse of treated water in agricultural purposes (Priac et al., 2017; D. Wu et al., 2018). Natural adsorbents are environmentally friendly, inexhaustible, and of low cost which can either be reused or simply disposed of by incineration (Rangabhashiyam et al., 2019).

Lichens have been inducted in the biomonitoring process for metal contamination (Kłos et al., 2018) as they effectively reflect integrated long-term accumulation, and not necessarily short-term patterns (Garty, 2002). Lichens have also been found to bind metals in a strongly pH-dependent manner, which can be extrapolated to make use of lichen biomass as an adsorbent for the removal of heavy metal from industrial effluent (Şenol et al., 2019). However, the metal biosorption potential of dried lichen biomass has been tested in very limited studies (Pipíška et al., 2008).

Parmotrema tinctorum has been used as spice and flavoring agents among some ethnic groups in India (Upreti et al., 2005). Cobalt adsorption by *P. tinctorum* foliose has been effective under acidic conditions with a maximum adsorption capacity of 22.10 mg g^{-1} (Ohnuki et al., 2003). *P. tinctorum* can accumulate Pu(VI) and U(VI) on the upper and lower surfaces and in cortical and medullary layers (Jabbar & Wallner, 2015).

However, in absence of any credible report on nickel adsorption by the lichen, the present study investigates the efficiency of *P. tinctorum* on nickel removal from wastewater effluent adopting batch studies under different operating conditions. Experiments were carried out to establish relevant adsorption kinetics and maximum adsorption capacity from isotherms analysis. The attenuation of metal toxicity in wastewater, following the biosorption process, was evaluated against soil microorganisms and changes in seed germination patterns in phytotoxicity assay.

2 Materials and Methods

2.1 Collection of Industrial Wastewater

The raw effluent from the metal finishing industry was collected from Villangudi, a village in Madurai

district, Tamil Nadu, India. Following sedimentation, the wastewater supernatant was collected, filtered (0.45 μm), and stored for further studies.

2.2 Collection and Preparation of Biosorbent

The biomass of *Parmotrema tinctorum* (Despr. ex Nyl.) Hale, used as a biosorbent, was collected from Dr. Vinayaka, K. S., lichen taxonomist from Shimoga, Karnataka, India. About 70 g of biomass was taken, washed in deionized water, and dried in a hot air oven at 80 °C for 48 h. The dried biomass was grounded to a fine powder, sieved to 100 mesh sizes (150 μm), transferred into a polythene packet, and stored in a cool and dry place.

2.3 Nickel Biosorption with *Parmotrema tinctorum*

2.3.1 Optimal Adsorption Conditions

All adsorption parameters were measured in a batch system using diluted effluent from metal finishing industries in deionized water. The effects of initial pH (3–8), agitation speed (100–350 rpm), and incubation time (30–180 min) on Ni biosorption were examined. Solution pH values beyond pH 8 were not considered to avoid the formation of insoluble $\text{Ni}(\text{OH})_2$ (S. Singh & Shukla, 2017). Batch adsorption experiments were carried out in 100 ml conical flasks containing 50 ml Ni spiked solution (100 mg l^{-1}) and 2 g l^{-1} of biomass. Unless otherwise specified, experiments were conducted at pH 7.0, 30 °C, incubated at 300 rpm for 120 min, as the reference condition. Samples were withdrawn at predetermined time intervals and centrifuged at $5000 \times g$ for 10 min. The residual metal concentration of the supernatant was determined by atomic absorption spectroscopy (AAS) with Varian AA240 spectrometer. The average of triplicates has been reported in data analysis. The amount of heavy metal adsorbed was calculated using the following equation

$$q_e = \frac{(C_0 - C_e)}{M} \quad (1)$$

where q_e is the amount of metal adsorbed per unit mass of adsorbent (i.e., mg g^{-1}). C_0 and C_e are the

initial and residual concentrations of metal ions (mg l^{-1}) before and after adsorption, respectively. V is the volume of the adsorption medium (l), and M is the mass of the adsorbent (g).

The removal efficiency is calculated as in Eq. 2.

$$\text{Removal efficiency}(\%) = \frac{C_0 - C_e}{C_0} \times 100 \quad (2)$$

where C_t is the aqueous phase metal concentration at any given time t .

2.3.2 Adsorption Isotherm

Isotherm studies were conducted in a series of 100 ml stoppered conical flasks containing diluted metal solutions. In the experimental sets, an initial dose of metal ion concentration was fixed at 100 mg l^{-1} , while varying the biosorbent dose between 2 and 5 g l^{-1} . The pH, agitation speed, and incubation time were invariant across the sets. After incubation, sample solutions were separated from biosorbent by centrifugation at $5000 \times g$ for 10 min, and residual nickel concentration in supernatants was measured.

The equilibrium data for metal adsorption were analyzed using four different isotherm models: Langmuir, Freundlich, Temkin, and Dubinin–Radushkevich (D-R) isotherms. Langmuir isotherm assumes monolayer sorption onto a fixed number of equivalent binding sites without any interaction between adsorbate molecules and is represented by Eq. 3.

$$q_e = \frac{q_m K_l C_e}{1 + K_l C_e} \quad (3)$$

where q_e is the amount of nickel adsorbed (mg g^{-1}) on the adsorbent surface at equilibrium, C_e is the equilibrium nickel concentration (mg l^{-1}), q_m is the maximum adsorption capacity (mg g^{-1}), and K_l is the Langmuir constant related to binding strength (l mg^{-1}).

The Freundlich isotherm is an empirical equation for multilayer, heterogeneous adsorption sites and is given by Eq. 4.

$$q_e = K_f C_e^n \quad (4)$$

The adjustable parameters, K_f denotes the adsorption capacity and n is the heterogeneity factor related

to the intensity of adsorption, where $n < 1$ describes favorable adsorption.

The Temkin isotherm considers indirect adsorbate/adsorbate interactions on the adsorption process and is given by Eq. 5.

$$q_e = B \ln A + B \ln C_e \quad (5)$$

where $B = RT/b$ represents Temkin constant; A (l g^{-1}) is Temkin adsorption potential. Required parameters (from the models) were obtained from non-linear least-square regression where sum of square error between experimental and modelled q_e values was minimized while iterating the parametric guess values using *fmincon* algorithm in Matlab 2018b (Math-Works®). Parameter confidence intervals were also estimated using a non-parametric bootstrapped resampling procedure. These parameters were interpreted to determine the models that suitably described the adsorption process.

D-R isotherm does not assume a homogeneous surface and provides an insight on the nature of adsorption, i.e., whether physical or chemical one (Ayawei et al., 2017; Inyinbor et al., 2016). The linear form of the D-R isotherm is expressed as in Eq. 6

$$\ln(q_e) = \ln(q_m) - k\varepsilon^2 \quad (6)$$

where q_e is the amount of Ni adsorbed per unit weight of adsorbent (mg/g), q_{max} is the maximum adsorption capacity (mg/g), k is the constant related to the sorption energy (mol^2/J^2), and ε is the Polanyi potential, which is given by Eq. 7 (Hu & Zhang, 2019)

$$\varepsilon = RT \ln \left(1 + \frac{1}{C_e} \right) \quad (7)$$

where R is the gas constant ($8.314 \text{ J/mol} \cdot \text{K}$) and T is the temperature (K). The mean energy of sorption E (kJ/mol) is calculated by Eq. 8.

$$E = \frac{1}{\sqrt{2k}} \quad (8)$$

Energies of absorption values between 1 and 8 kJ/mol indicate a physisorption, while energies between 9 and 16 kJ/mol are characteristic of chemisorption process (Nishikawa et al., 2018).

2.3.3 Adsorption Kinetics

The experiments were conducted in 100 ml stoppered conical flasks containing 50 ml of Ni spiked solution (100 mg l^{-1}) at its native pH of 7.0, with 2 g l^{-1} biosorbent. The experimental sets were incubated at a constant agitation speed of 300 rpm at room temperature. Samples were withdrawn from different experimental sets after an incubation period of 30, 60, 90, 120, 150, and 180 min. Samples were immediately filtered, and nickel concentration was measured using AAS.

The movement of metal ions from the bulk of the solution to adsorbent can be neglected in the well-agitated system and the process can be regulated by boundary layer diffusion and/or binding to a specific adsorption site (Burks et al., 2014). A pseudo-first-order (PFO), pseudo-second-order (PSO), and intraparticle diffusion (IPD) models (Eqs. 9–11) were probed to describe the kinetics.

$$q_t = q_e (1 - e^{-k_1 t}) \quad (9)$$

$$\left(\frac{1}{q_t} - \frac{1}{q_e} \right) t = \frac{1}{k_2 q_e^2} \quad (10)$$

$$q_t = k_i t^{0.5} \quad (11)$$

where k_1 , k_2 , and k_i are rate constants of adsorption in PFO (min^{-1}), PSO ($\text{g mg}^{-1} \text{ min}^{-1}$), and IPD ($\text{mg g}^{-1} \text{ min}^{-0.5}$) models, respectively. The adsorption capacity (mg g^{-1}) measured at time t is q_t .

2.4 Biomass Characterization Pre- and Post-adsorption

2.4.1 X-ray Diffraction (XRD)

The *P. tinctorum* biomass before and after nickel (II) ion adsorption was examined using an X-ray diffractometer (RIGAKU, Ultima – III, Japan) with a $\text{Cu K}\alpha$ X-ray source ($\lambda = 0.15406 \text{ nm}$, 40 kV). The sample was scanned between 2θ of $10\text{--}90^\circ$ using a continuous scan mode at a scanning speed of $10^\circ \text{ min}^{-1}$.

2.4.2 Fourier Transform Infrared (FTIR) Spectroscopy

The FTIR spectra of both pristine and nickel (II) treated biosorbent were recorded in the transmission mode between 4000 and 500 cm^{-1} at room temperature using KBr pellet at a resolution of 4 cm^{-1} (Shimadzu, Prestige-21, Japan).

2.5 Attenuation of Nickel Toxicity in Treated Wastewater

2.5.1 Microbial Toxicity

The attenuation of toxicity in the biosorption process, if any, was verified with two agriculturally important microorganisms, i.e., *Phosphobacter* sp. and *Azospirillum* sp. (Souza et al., 2015). Freshly grown (4 h) bacterial culture of those indicator species was transferred onto Mueller–Hinton agar plates using sterile cotton swabs. Untreated or biosorbent treated water samples containing reference nickel concentrations of 40, 50, 60, and 70 mg l^{-1} were added (100 μl) into 2 mm diameter wells punctured into the agar. Plates were incubated at 37 $^{\circ}\text{C}$ for 24 h and subsequently examined for the zone of inhibition.

2.5.2 Phytotoxicity in Seed Germination and Plant Growth

The soil used in the greenhouse experiment was collected from about 2 cm depth in and around Karunya University campus, Coimbatore, after removal of the surface vegetation. The soil (42.5% clay, 45.3% silt, and 12.2% sand) was air-dried, sieved to less

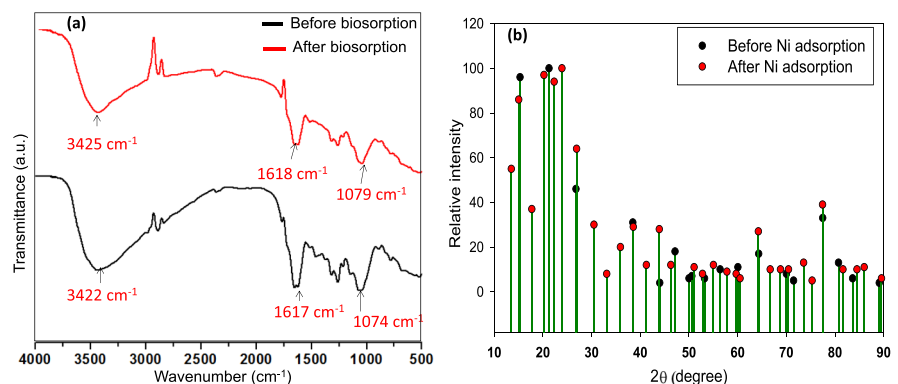
than 2 mm, and sterilized by autoclaving at 120 $^{\circ}\text{C}$ for 20 min for three consecutive days. Phytotoxicity experiments were conducted in 5000 cm^3 pots, with 2 kg of sterilized soil adjusted to 66% of its water holding capacity, in a greenhouse controlled climatic conditions (18–25 $^{\circ}\text{C}$). *Vigna radiata* seeds collected from the local market were surface sterilized (soaking in 2.5% sodium hypochlorite for 5 min), washed with distilled water, and placed into soil pots (6 seeds in each pot). Two different treatments were adopted, i.e., pots were daily irrigated with (i) biosorbent treated wastewater (mixed with 5 g l^{-1} of *P. tinctorum* biomass for 3 h at 300 rpm and filtered) and (ii) untreated wastewater, and germination rate, growth were recorded after 7 days.

3 Results and Discussion

3.1 Biomass Characterization Before and After Ni Biosorption

FTIR spectroscopy was used to identify functional groups present in the biomass, promoting the adsorption of the Ni (II) ions from the aqueous solution as in Fig. 1a. Presence of a broad intense band at $\sim 3400 \text{ cm}^{-1}$ indicates the presence of O–H stretching vibration due to hydroxyl and carboxyl groups (Khajavian et al., 2019). A peak at 1617 cm^{-1} suggests asymmetric stretching of the carboxylic (C=O) double bond on biomass surface (Mohammed et al., 2019), which remains nearly unaffected (1618 cm^{-1}) following Ni adsorption. Absorbance intensity in the range 1000–1100 cm^{-1} is a characteristic fingerprint

Fig. 1 The change in **a** FTIR and **b** XRD absorption pattern for *P. tinctorum* biomass following Ni adsorption



region for polysaccharides due to vibration modes of COC=bonds. The absorbance band positioned at 1074 cm^{-1} and 3422 cm^{-1} in *P. tinctorum* biomass shifted to 1079 cm^{-1} and 3425 cm^{-1} , respectively, following Ni (II) adsorption. Shift of absorbance band from ~ 1074 (related to amide or phosphate groups) to 1079 cm^{-1} has also been reported in fungal biomass following Ni adsorption (Enayatizamir et al., 2020). The slight shifts in the peaks of functional groups following Ni (II) adsorption reflect the binding or attachment of metal ions on the cell walls of *P. tinctorum* biomass (Sharma et al., 2021), possibly through ion exchange mechanism (S. A. Singh & Shukla, 2016; S. Singh & Shukla, 2017). However, possibility of any chemical interaction can be rejected (Sari et al., 2007). Similar observations have been made in other studies, and those

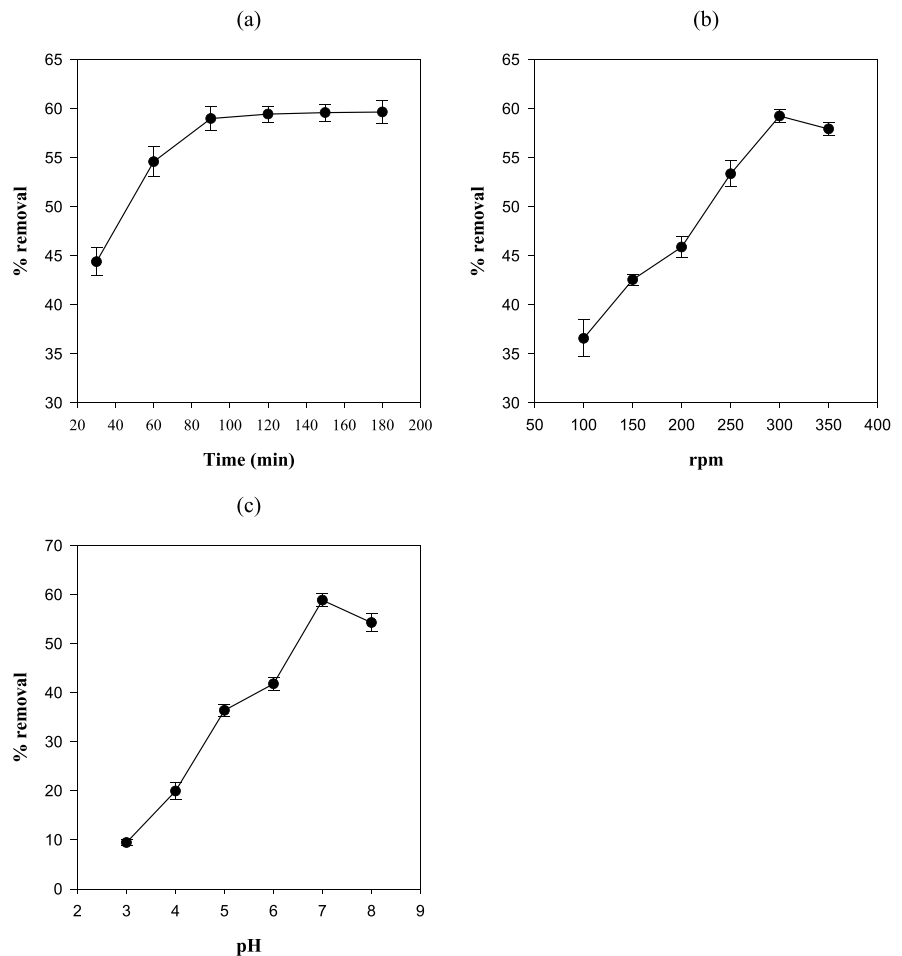
detailed features of the IR spectrum differ depending on the biomass involved (Herrera-Barros et al., 2020).

The XRD of original and nickel adsorbed *P. tinctorum* biomass is shown in Fig. 1b. The existence of XRD peak at 2θ of 15.28° (biomass) and 15.02° (Ni adsorbed biomass) is an amorphous form of the cellulose family. Similarly, XRD peaks at 21.24° and 20.20° are suggestive of cellulose family crystalline phases (Kardam et al., 2014).

3.2 Effect of Operating Parameters on Nickel Biosorption

The results of Ni (II) adsorption as a function of time from the biosorption study are shown in Fig. 2a. It revealed that the extent of adsorption increased rapidly during the initial stage and then became slower at a later stage till the equilibrium is attained. It should

Fig. 2 Effect of **a** incubation time, **b** stirring speed (rpm), and **c** initial pH of solution on nickel biosorption by *P. tinctorum*. The reference condition: biomass, 2 g l^{-1} ; initial nickel concentration, 100 mg l^{-1} ; pH, 7; stirring speed, 300 rpm; and incubation time, 120 min



be noted that though 44% of the Ni (II) was adsorbed within 30 min, an equilibrium adsorption of about 59.66% was reached nearly after 180 min. These assessments on equilibrium time are important to design wastewater treatment applications.

The effect of agitation speed in the range of 100–350 rpm was studied for *P. tinctorum* mediated Ni removal (Fig. 2b). The rate of adsorption is controlled by either film diffusion or pore diffusion, depending on the amount of agitation in the system. The extent of biosorption increased with stirring speed between 100 and 300 rpm, possibly due to a decrease in boundary layer thickness, reduction in surface film resistance, and increase in mass transfer rate. At 350 rpm, the biosorption efficiency was found to be slightly lower, possibly to inadequate contact between Ni (II) ions and binding sites due to vortex formation at high agitation speeds (Long et al., 2018).

The effect of pH on the biosorption of nickel onto *P. tinctorum* biomass was studied in the range pH 3 to pH 8. Figure 2c shows the effect of pH on Ni (II) adsorption, where maximum removal of 58.89% was achieved at pH 7. At lower pH values (i.e., pH < 7), Ni (II) adsorption by *P. tinctorum* biomass steadily declined. This could possibly be attributed to increased competition between hydrogen and nickel ions for adsorption sites (Krika et al., 2016). As the pH increases, the active sites of the biosorbent become negatively charged and able to bind positive metal ions in solution (Shweta Gupta & Kumar, 2019). However, optimal pH for Ni adsorption has been shown to vary in literature depending on cat-achrestic biosorbent (Herrera-Barros et al., 2020; Sudha et al., 2015). The decrease in nickel absorption at pH 8 in the present study may be associated formation of a metal ion complex with the hydroxide ion (OH⁻) in the aqueous or metal ion precipitation (Foroutan et al., 2019). The dependency of Ni (II) adsorption on pH suggests electrostatic adsorption or surface precipitation as the predominant mechanism, though cation exchange and surface complexation cannot be ruled out (Shen et al., 2017).

3.3 Adsorption Isotherm

The fitness of Langmuir, Freundlich, Temkin, and D-R isotherms for Ni (II) adsorption on biomass adopting non-linear approach is shown in Fig. 3, and corresponding isotherm parameters along with

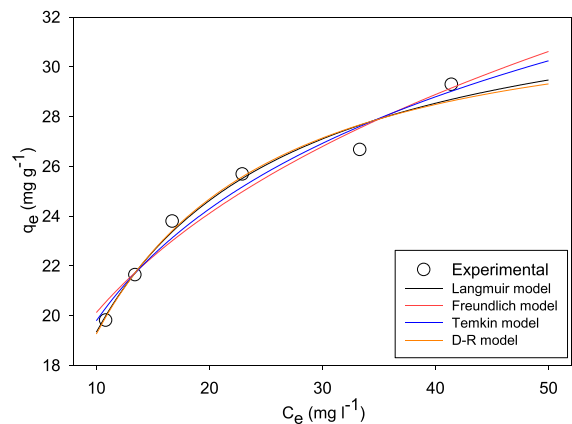


Fig. 3 The isotherms for Ni (II) adsorption onto *P. tinctorum* biomass as evaluated with non-linear Langmuir, Freundlich, Temkin, and D-R isotherm models

regression coefficients are presented in Table 1. Though all the four isotherm accounts the adsorption reasonably well, the regression coefficient for Langmuir model is marginally better (R^2 , 0.974) than the others. The confidence intervals for the parameter estimates and regression coefficients, using the non-parametric bootstrap resampling approach, also suggest the same. The q_m and K_L estimates for the Langmuir model through non-linear least-square regression were 33.92 mg g⁻¹ and 0.13 l mg⁻¹, respectively.

The Langmuir model assumes a homogeneous adsorption site without any putative interaction between the adsorbed Ni (II) on the nearby free adsorption sites. A dimensionless constant, referred as separation factor, formalized from Langmuir model, i.e., $R_L = 1/(1 + C_0 K_L)$, can be used to characterize whether an adsorption system is “favorable” or “unfavorable” (Hall et al., 1966). Calculated R_L value of 0.070 in present isotherm analysis suggests favorable adsorption behavior (Ahmadi et al., 2016). The estimated Freundlich model parameter $n < 1$ also suggests the physisorption process (Foroutan et al., 2017).

The least-square estimates of maximum Ni (II) adsorption capacity (q_m) and adsorption free energy (E) using non-linear D-R adsorption model were 31.78 mg l⁻¹ and 4.74 kJ mol⁻¹, respectively. The result suggests role of physisorption behind the nickel adsorption by *P. tinctorum* biomass. Other studies have also reported physisorption of Ni (II)

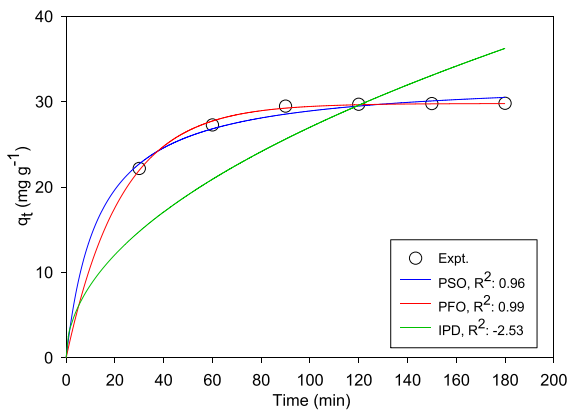
Table 1 Isotherm parameters on adsorption of Ni (II) onto *P. tinctorum* biomass

Parameters	Isotherm models ^a											
	Freundlich			Langmuir			Temkin			D-R model		
	K_f	n	R^2	K_L	q_m	R^2	A	B	R^2	E	q_m	R^2
Estimate	11.04	0.26	0.96	0.13	33.92	0.97	2.11	6.50	0.97	4.74	31.78	0.97
Lower CI ^b	9.27	0.22	0.94	0.11	32.14	0.96	1.29	5.56	0.95	4.44	30.53	0.95
Upper CI ^b	12.65	0.30	1.00	0.16	35.59	1.00	3.95	7.43	1.00	5.11	32.86	0.98

Estimates of best-fit model parameters are shown in boldface

^aModel parameter unit: K_f ($l\ g^{-1}$); K_L ($l\ mg^{-1}$); q_m ($mg\ g^{-1}$); A ($l\ g^{-1}$); E (kJ/mol)

^bConfidence intervals are based on 5000 non-parametric bootstrap sampling

**Fig. 4** Ni (II) adsorption kinetics using *P. tinctorum* biomass using PFO, PSO, and IPD models

from aqueous solution using lignocellulosic biomass (Chanda et al., 2021) and activated carbon (Abd El-Magied et al., 2018). Gupta et al. (2019) observed nickel adsorption onto modified *Aloe vera* leaf powder to be a physisorption process with mean free energy of $2.88\ kJ\ mol^{-1}$. Adsorption forces in physisorption are weak permitting fast attainment of equilibrium (U. Kumar, 2011). Studies also suggest that mode of sorption of Ni (II) onto biomass carbon could be physisorption, ion exchange, or chemisorption, depending on prevailing sorption conditions (Nnaji et al., 2021).

3.4 Kinetics of Biosorption

The experimental data for Ni (II) adsorption onto *P. tinctorum* fitted well with PFO as well as PSO kinetics (Fig. 4). The values of q_e calculated from these models were compared with experimental q_e values

Table 2 Kinetic constants for Ni (II) adsorption on *P. tinctorum* biomass using PFO, PSO, and IPD models

Kinetic model	Expt. q_e ($mg\ g^{-1}$)	Kinetic parameters		
		q_e ($mg\ g^{-1}$)	k_1, k_2, k_i	R^2
PFO	29.83	29.82	0.044	0.993
PSO	29.83	32.78	0.002	0.956
IPD	-	-	2.70	-2.535

* k_1 : min^{-1} , k_2 : $g\ mg^{-1}\ min^{-1}$, k_i : $mg\ g^{-1}\ min^{-0.5}$

(Table 2). It was observed that the values of experimental and modelled q_e are very similar in PFO model whereas they differed appreciably in PSO model. The regression coefficient (R^2) for the PFO model (0.993) is higher as compared to that of PSO model (0.956). The IPD model failed to fit the data for adsorption kinetics ($R^2 = -2.535$).

The kinetics of the adsorption process is governed by the efficiency of the steps involved in the movement of adsorbate to the adsorbent surface, diffusion to surface pores, particle, and binding to active sites. As multiple events take place simultaneously or sequentially, of which some could be slower than others, the overall kinetics may be explained with more than one kinetic model (Şenol et al., 2021). Among the different adsorption kinetic models, PFO, and even to a greater extent PSO model, has gained popularity in biosorption systems. Linearization of PFO (which is often the case) introduces discontinuity at equilibrium, making the linearized PSO a better choice even for datasets that inherently fit PFO (Revellame et al., 2020).

Ni biosorption could follow either PFO or PSO kinetics depending on the physical state of biomass. For example, Işik (2008) observed Ni adsorption

to be PFO for non-living biomass, whereas for living biomass, the PSO kinetic was more appropriate. The author suggested the involvement of different metal uptake processes, i.e., intracellular uptake in viable cells, in addition to the passive uptake onto the cell surface of both viable and non-viable cells. PFO adsorption model is based on the sorption capacity of solids in solid–liquid systems where adsorbate moves only to unoccupied adsorption sites (Jiao Wang et al., 2015). On the other hand, PSO adsorption kinetics could be attributed to the chemisorption process through the formation of covalent bonds (Ezeonuegbu et al., 2021).

3.5 Comparison of Biosorption Capacity

The Ni (II) biosorption by different bacterial, fungal, algal, and lignocellulosic biomass in other reported studies is included in Table 3, for comparison. It is evident that Ni adsorption capacity varied significantly across different biosorbents. For example, in algal species, the adsorption capacity varied between 3.72 and 52 mg g⁻¹. The maximum Ni (II) capacity by *P. tinctorum* in this study is better than other lichen biomass such as 9.71 mg g⁻¹ by *Ramalina fraxinea* (Candan et al., 2017), or 7.9 mg g⁻¹ by *Cladonia furcata* (Sarı et al., 2007), but inferior to *Diploicia canescens* which can adsorb about 66.7 mg g⁻¹ at pH 5 (Hannachi & Boubaker, 2016). In most of the referred

Table 3 The comparison of Ni (II) removal efficiency for biosorbents reported in literature

Type	Biosorbent	Optimal condition	Choice of isotherm	q_m (mg/g)	References
Algae	<i>Cystoseria indica</i>	25 °C, pH 6	Freundlich	18.17	(Khajavian et al., 2019)
Algae	<i>Durvillaea antarctica</i>	pH 5.0	Sips	32.85	(Guarín-Romero et al., 2019)
Algae	<i>Sargassum</i> sp.	30 °C, pH 5	Langmuir	52 ^a	(Barquilha et al., 2017)
Algae	<i>Chrysophyta</i> , <i>Chlorophyte</i> , <i>Cyanophyta</i>	pH 7	Temkin	9.85	(Mohammed et al., 2019)
Algae	<i>Chara</i> sp.	pH 5	Langmuir	3.72	(Kalash et al., 2020)
Algae	<i>Scenedesmus obliquus</i>	30 °C, pH 7	Langmuir	25.76	(Akhtari et al., 2021)
Algae	<i>Sargassum hemiphyllum</i>	35 °C, pH 4–8	Langmuir	42.9	(Fan et al., 2019)
Bacteria	<i>Arthrospira platensis</i>	pH 4.0	Langmuir	13.4	(Zinicovscaia et al., 2018)
Bacteria	<i>B. cereus</i>	Unknown	Langmuir	50.2	(Kashyap et al., 2021)
Bacteria	<i>Streptomyces roseorubens</i> SY	40 °C, pH 5	Langmuir	208	(Long et al., 2018)
Bacteria	<i>Planococcus</i> sp.	n.a	Langmuir	34	(Hoseini et al., 2020)
Bacteria	<i>Brevibacterium</i> sp.	n.a	Langmuir	101	(X. Wu et al., 2021)
Fungi	<i>P. chrysosporium</i>	36 °C, pH 6	Langmuir	46.5	(Noormohamadi et al., 2019)
Fungi	<i>Penicillium</i> sp.	pH 5.5	Freundlich	63.6	(Sundararaju et al., 2020)
Fungi	<i>A. flavus</i> , <i>N. crassa</i>	pH 5–6	Langmuir	4.5, 3.68	(Sharma et al., 2021)
Fungi	<i>A. oryzae</i> , <i>A. clavatus</i> , <i>A. fumigatus</i>	38 °C	Langmuir	0.94, 1.0, 1.30	(Gunjal, 2021)
Agricultural waste	Acorn shell — <i>Quercus crassipes</i>	pH 8	Freundlich	104	(Aranda-García & Cristiani-Urbina, 2018)
Agricultural waste	Alkali-modified lemon peel	pH 5	Langmuir	36 ^a	(Villen-Guzman et al., 2021)
Agricultural waste	Sugarcane bagasse	30 °C, pH 6	Freundlich	123.46	(Ezeonuegbu et al., 2021)
Agricultural waste	<i>Swietenia macrophylla</i> sawdust	25 °C, pH 9	Langmuir	13.42	(Chanda et al., 2021)
Lichen	<i>P. tinctorum</i>	pH 7	Langmuir	33.92	This study

LC, lignocellulosic or plant-based

^aAuthor reported q_m values were in mmol g⁻¹

studies, the optimal biosorption condition has been reported to be in moderately acidic, possibly to avoid unfavorable competition with hydrogen ions under strong acidic pH, or hydroxide complexes or causing precipitation in alkaline pH (Şenol et al., 2021).

3.6 Microbial Toxicity

Different dilutions of untreated effluent wastewater, from the metal finishing industry, inhibited the growth of agriculturally important microorganisms, viz. *Phosphobacter* sp. and *Azospirillum* sp., as reflected from a clear zone of inhibition as shown in Fig. 5 and Table 4. However, no zone of inhibition was observed when biosorbent treated water was used. The toxicity of untreated effluent increased with an increase in Ni (II) concentrations. Fungal treatment mediated toxicity attenuation of dye on various microbial culture has been studied, but

Table 4 Microbial toxicity of treated and untreated metal finishing effluent against *Azospirillum* sp. and *Phosphobacter* sp

Conc. of Ni (II) in sample (mg l ⁻¹)	Zone of inhibition on Petri plate (mm) ^a			
	<i>Phosphobacter</i> sp.		<i>Azospirillum</i> sp.	
	Untreated WW	Treated WW	Untreated WW	Treated WW
40	17	n.d	18	n.d
50	18	n.d	20	n.d
60	20	n.d	22	n.d
70	21	n.d	24	n.d

^an.d., no significant zone of inhibition

there is no report on soil microorganisms as test subject.

In this study, the untreated metal finishing effluent was toxic and their toxic effects increased with the increase in concentration.

Fig. 5 Effect of treated (left quadrants) and untreated (right quadrants) wastewater effluent on the growth of **a, b** *Phosphobacter* sp. and **c, d** *Azospirillum* sp. in agar well diffusion assay. The numeral near the wells indicates the volume (40, 50, 60, 70 µl) of treated or untreated water loaded

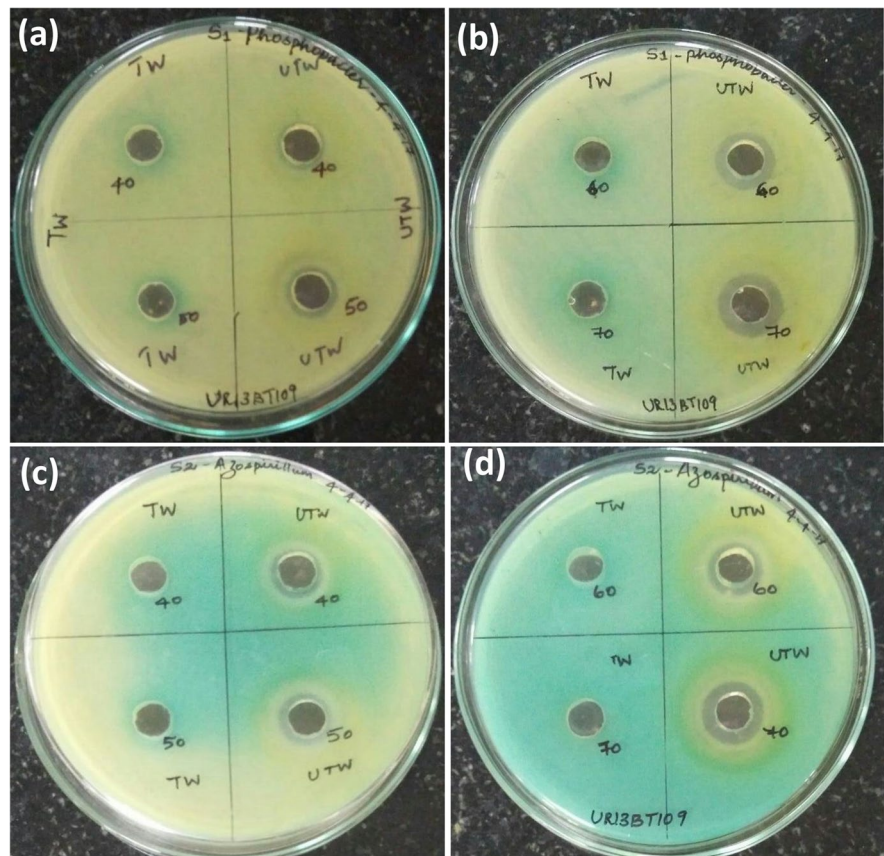
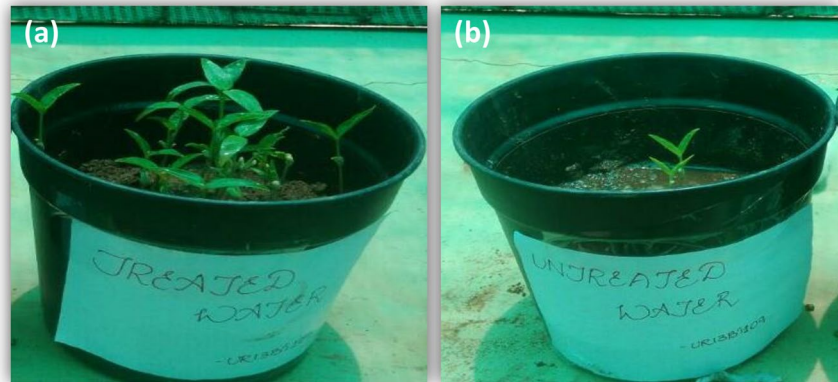


Fig. 6 Seed germination in greenhouse experimental sets (day 7) irrigated with **a** biosorbent treated and **b** raw untreated metal finishing effluent



3.7 Study on Seed Germination Effect

Similarly, a comparison study on treated and untreated water based on the seed germination effect was studied using *Vigna radiata* seed, since industrial wastewater is typically more toxic for agricultural purposes. Two out of six seeds germinated on day 3 when irrigated with untreated wastewater. However, in case of treated water group, 100% germination was observed. The high inhibiting effects with untreated effluent could be related to increase osmotic stress due to high level of heavy metals (Kaboosi, 2017). Moreover, plant growth was evidently better in treated water set, when recorded on 7th day (Fig. 6). The results clearly suggest attenuation of phytotoxicity for metal finishing effluent following biosorption with *P. tinctorum* biomass.

4 Conclusions

Biomass of *P. tinctorum* can effectively remove Ni (II) from metal finishing effluent with a maximum adsorption capacity of 33.923 mg g^{-1} . The adsorption process is dependent on pH of the medium and follows Langmuir isotherm of favorable physisorption. Reduction of microbial toxicity and phytotoxicity of metal finishing effluent were evident when the wastewater was pretreated with *P. tinctorum* biomass. Though the study opens up the possibility of using *P. tinctorum* biomass to treat metal finishing industries wastewater for agricultural repurposing, comprehensive tired toxicity analysis is warranted in this direction.

Author Contribution SM conceived the project work and drafted the outline of the manuscript. ZKG and MP performed different laboratory experiments, and created the initial draft. RN characterized the *P. tinctorum* biomass. BM revised the manuscript, redrawn the artwork, and performed mathematical analysis, and reshaping the discussion. SM supervised the experimental work and along with VKS revised the manuscript. All the authors cross-checked the content, updated, and edited the manuscript. All authors agree to the submission.

Funding This work is supported by the Karunya Institute of Technology and Sciences, Coimbatore, India.

Data Availability Experimental data can be available from corresponding authors on reasonable request.

Declarations

Ethical Approval Ethical approval not required. Standard ethical and professional conduct have been followed.

Consent to Participate Not applicable as involved no human participants.

Consent to Publish Not applicable.

Competing Interests The authors declare no competing interests.

References

- Abd El-Magied, M. O., Hassan, A. M. A., Gad, H. M. H., Mohammed, T. F., & Youssef, M. A. M. (2018). Removal of nickel (II) ions from aqueous solutions using modified activated carbon: A kinetic and

- equilibrium study. *Journal of Dispersion Science and Technology*, 39(6), 862–873. <https://doi.org/10.1080/01932691.2017.1402337>
- Ahmadi, M., Kouhgardi, E., & Ramavandi, B. (2016). Physico-chemical study of dew melon peel biochar for chromium attenuation from simulated and actual wastewaters. *Korean Journal of Chemical Engineering*, 33(9), 2589–2601. <https://doi.org/10.1007/s11814-016-0135-1>
- Akhtari, N., Sadeghi, M. S., & Agah, H. (2021). Biosorption of nickel ions by *Scenedesmus obliquus* from aqueous solution. *Journal of Water and Wastewater Science and Engineering*, 6(1), 41–51. <https://doi.org/10.22112/jwwse.2020.229584.1205>
- Aranda-García, E., & Cristiani-Urbina, E. (2018). Kinetic, equilibrium, and thermodynamic analyses of Ni(II) biosorption from aqueous solution by acorn shell of *Quercus crassipes*. *Water, Air, & Soil Pollution*, 229(4), 119. <https://doi.org/10.1007/s11270-018-3775-4>
- Ayawei, N., Ebelegi, A. N., & Wankasi, D. (2017). Modeling and interpretation of adsorption isotherms. *Journal of Chemistry*, 2017, 1–11. <https://doi.org/10.1155/2017/3039817>
- Barquilha, C. E. R., Cossich, E. S., Tavares, C. R. G., & Silva, E. A. (2017). Biosorption of nickel(II) and copper(II) ions in batch and fixed-bed columns by free and immobilized marine algae *Sargassum* sp. *Journal of Cleaner Production*, 150, 58–64. <https://doi.org/10.1016/j.jclepro.2017.02.199>
- Burks, T., Avila, M., Akhtar, F., Göthelid, M., Lansåker, P. C., Toprak, M. S., et al. (2014). Studies on the adsorption of chromium(VI) onto 3-mercaptopropionic acid coated superparamagnetic iron oxide nanoparticles. *Journal of Colloid and Interface Science*, 425, 36–43. <https://doi.org/10.1016/J.JCIS.2014.03.025>
- Buxton, S., Garman, E., Heim, K. E., Lyons-Darden, T., Schlekat, C. E., Taylor, M. D., & Oller, A. R. (2019). Concise review of nickel human health toxicology and ecotoxicology. *Inorganics*, 7(7), 89. <https://doi.org/10.3390/inorganics7070089>
- Candan, M., Tay, F., Avan, I., & Tay, T. (2017). Removal of copper(II) and nickel(II) ions from aqueous solution using non-living lichen *Ramalina fraxinea* biomass: Investigation of kinetics and sorption isotherms. *Desalination and Water Treatment*, 75, 148–157. <https://doi.org/10.5004/dwt.2017.20749>
- Chanda, R., Mithun, A. H., Hasan, M. A., & Biswas, B. K. (2021). Nickel removal from aqueous solution using chemically treated mahogany sawdust as biosorbent. *Journal of Chemistry*, 2021, 1–10. <https://doi.org/10.1155/2021/4558271>
- CPCB. (2012). *Effluent and emission standard*.
- Duong, H. C., Pham, T. M., Luong, S. T., Nguyen, K. V., Nguyen, D. T., Ansari, A. J., & Nghiem, L. D. (2019). A novel application of membrane distillation to facilitate nickel recovery from electroplating wastewater. *Environmental Science and Pollution Research*, 26(23), 23407–23415. <https://doi.org/10.1007/s11356-019-05626-9>
- Enayatizmir, N., Liu, J., Wang, L., Lin, X., & Fu, P. (2020). Coupling Laccase production from *Trametes pubescens* with heavy metal removal for economic waste water treatment. *Journal of Water Process Engineering*, 37, 101357. <https://doi.org/10.1016/j.jwpe.2020.101357>
- Ezeonuegbu, B. A., Machido, D. A., Whong, C. M. Z., Japhet, W. S., Alexiou, A., Elazab, S. T., et al. (2021). Agricultural waste of sugarcane bagasse as efficient adsorbent for lead and nickel removal from untreated wastewater: Biosorption, equilibrium isotherms, kinetics and desorption studies. *Biotechnology Reports*, 30, e00614. <https://doi.org/10.1016/j.btre.2021.e00614>
- Fan, X., Xia, J., & Long, J. (2019). The potential of nonliving *Sargassum hemiphyllum* as a biosorbent for nickel(II) removal-isotherm, kinetics, and thermodynamics analysis. *Environmental Progress & Sustainable Energy*, 38(s1), S250–S259. <https://doi.org/10.1002/ep.12997>
- Foroutan, R., Esmaeili, H., Rishehri, S. D., Sadeghzadeh, F., Mirahmadi, S., Kosarifard, M., & Ramavandi, B. (2017). Zinc, nickel, and cobalt ions removal from aqueous solution and plating plant wastewater by modified *Aspergillus flavus* biomass: A dataset. *Data in Brief*, 12, 485–492. <https://doi.org/10.1016/j.dib.2017.04.031>
- Foroutan, R., Mohammadi, R., Farjadfar, S., Esmaeili, H., Saberi, M., Sahebi, S., et al. (2019). Characteristics and performance of Cd, Ni, and Pb bio-adsorption using *Callinectes sapidus* biomass: Real wastewater treatment. *Environmental Science and Pollution Research*, 26(7), 6336–6347. <https://doi.org/10.1007/s11356-018-04108-8>
- Gad, S. C. (2014). Nickel and nickel compounds. In *Encyclopedia of toxicology* (pp. 506–510). Elsevier. <https://doi.org/10.1016/B978-0-12-386454-3.00889-7>
- Garty, J. (2002). Biomonitoring heavy metal pollution with lichens. In *Protocols in lichenology* (pp. 458–482). Berlin, Heidelberg: Springer Berlin Heidelberg. https://doi.org/10.1007/978-3-642-56359-1_27
- Gitet, H., Hilawie, M., Muuz, M., Weldegebriel, Y., Gebremichael, D., & Gebremedhin, D. (2016). Bioaccumulation of heavy metals in crop plants grown near Almeda Textile Factory, Adwa Ethiopia. *Environmental Monitoring and Assessment*, 188(9), 500. <https://doi.org/10.1007/s10661-016-5511-0>
- Guarín-Romero, J. R., Rodríguez-Estupiñán, P., Giraldo, L., & Moreno-Piraján, J. C. (2019). Simple and competitive adsorption study of nickel(II) and chromium(III) on the surface of the brown algae *Durvillaea antarctica* biomass. *ACS Omega*, 4(19), 18147–18158. <https://doi.org/10.1021/acsomega.9b02061>
- Gunjal, A. (2021). Study of Langmuir kinetics for removal of heavy metals by the fungal biomass. *Proceedings of the Indian National Science Academy*, 87(1), 107–109. <https://doi.org/10.1007/s43538-021-00011-y>
- Gupta, S., Satpati, S., Nayek, S., & Garai, D. (2010). Effect of wastewater irrigation on vegetables in relation to bioaccumulation of heavy metals and biochemical changes. *Environmental Monitoring and Assessment*, 165(1–4), 169–177. <https://doi.org/10.1007/s10661-009-0936-3>
- Gupta, Shweta, & Kumar, A. (2019). Removal of nickel (II) from aqueous solution by biosorption on *A. barbadensis* Miller waste leaves powder. *Applied Water Science*, 9(4), 96. <https://doi.org/10.1007/s13201-019-0973-1>
- Gupta, S., Sharma, S. K., & Kumar, A. (2019). Biosorption of Ni(II) ions from aqueous solution using modified *Aloe barbadensis* Miller leaf powder. *Water Science and*

- Engineering*, 12(1), 27–36. <https://doi.org/10.1016/j.wse.2019.04.003>
- Hall, K. R., Eagleton, L. C., Acrivos, A., & Vermeulen, T. (1966). Pore- and solid-diffusion kinetics in fixed-bed adsorption under constant-pattern conditions. *Industrial & Engineering Chemistry Fundamentals*, 5(2), 212–223. <https://doi.org/10.1021/i160018a011>
- Hannachi, Y., & Boubaker, T. (2016). Biosorption performance of the lichen biomass (*Diploicia canescens*) for the removal of nickel from aqueous solutions. *Desalination and Water Treatment*, 57(39), 18490–18499. <https://doi.org/10.1080/19443994.2015.1094424>
- Hemachandra, C. K., & Pathiratne, A. (2015). Assessing toxicity of copper, cadmium and chromium levels relevant to discharge limits of industrial effluents into inland surface waters using common onion, *Allium cepa* bioassay. *Bulletin of Environmental Contamination and Toxicology*, 94(2), 199–203. <https://doi.org/10.1007/s00128-014-1373-8>
- Herrera-Barros, A., Bitar-Castro, N., Villabona-Ortíz, Á., Tejada-Tovar, C., & González-Delgado, Á. D. (2020). Nickel adsorption from aqueous solution using lemon peel biomass chemically modified with TiO₂ nanoparticles. *Sustainable Chemistry and Pharmacy*, 17, 100299. <https://doi.org/10.1016/j.scp.2020.100299>
- Hoseini, A. A.-S., Kaboosi, H., Ahmady-Asbchin, S., Ghorbanalinezhad, E., & Peyravii Ghadikolaii, F. (2020). Binary biosorption of cadmium(II) and nickel(II) onto *Planococcus* sp. isolated from wastewater: Kinetics, equilibrium and thermodynamic studies. *Industrial Biotechnology*, 16(6), 386–393. <https://doi.org/10.1089/ind.2020.0021>
- Hu, Q., & Zhang, Z. (2019). Application of Dubinin-Radushkevich isotherm model at the solid/solution interface: A theoretical analysis. *Journal of Molecular Liquids*, 277, 646–648. <https://doi.org/10.1016/j.molliq.2019.01.005>
- Inyinbor, A. A., Adekola, F. A., & Olatunji, G. A. (2016). Kinetics, isotherms and thermodynamic modeling of liquid phase adsorption of Rhodamine B dye onto *Raphia hookeri* fruit epicarp. *Water Resources and Industry*, 15, 14–27. <https://doi.org/10.1016/j.wri.2016.06.001>
- İşik, M. (2008). Biosorption of Ni(II) from aqueous solutions by living and non-living ureolytic mixed culture. *Colloids and Surfaces B: Biointerfaces*, 62(1), 97–104. <https://doi.org/10.1016/j.colsurfb.2007.09.022>
- Jabbar, T., & Wallner, G. (2015). Biotransformation of radionuclides: Trends and challenges. In *Radionuclides in the environment* (pp. 169–184). Cham: Springer International Publishing. https://doi.org/10.1007/978-3-319-22171-7_10
- Javanbakht, V., Alavi, S. A., & Zilouei, H. (2014). Mechanisms of heavy metal removal using microorganisms as biosorbent. *Water Science and Technology*, 69(9), 1775–1787. <https://doi.org/10.2166/wst.2013.718>
- Kaboosi, K. (2017). The assessment of treated wastewater quality and the effects of mid-term irrigation on soil physical and chemical properties (case study: Bandargaz-treated wastewater). *Applied Water Science*, 7(5), 2385–2396. <https://doi.org/10.1007/s13201-016-0420-5>
- Kalash, K. R., Alalwan, H. A., Al-Furaiji, M. H., Alminshid, A. H., & Waisi, B. I. (2020). Isothermal and kinetic studies of the adsorption removal of Pb(II), Cu(II), and Ni(II) ions from aqueous solutions using modified *Chara* sp. algae. *Korean Chemical Engineering Research*, 58(2), 301–306. <https://doi.org/10.9713/kcer.2020.58.2.301>
- Kardam, A., Raj, K. R., Srivastava, S., & Srivastava, M. M. (2014). Nanocellulose fibers for biosorption of cadmium, nickel, and lead ions from aqueous solution. *Clean Technologies and Environmental Policy*, 16(2), 385–393. <https://doi.org/10.1007/s10098-013-0634-2>
- Kashyap, S., Chandra, R., Kumar, B., & Verma, P. (2021). Biosorption efficiency of nickel by various endophytic bacterial strains for removal of nickel from electroplating industry effluents: An operational study. *Ecotoxicology*. <https://doi.org/10.1007/s10646-021-02445-y>
- Khajavian, M., Wood, D. A., Hallajani, A., & Majidian, N. (2019). Simultaneous biosorption of nickel and cadmium by the brown algae *Cystoseria indica* characterized by isotherm and kinetic models. *Applied Biological Chemistry*, 62(1), 69. <https://doi.org/10.1186/s13765-019-0477-6>
- Khan, S., Anas, M., & Malik, A. (2019). Mutagenicity and genotoxicity evaluation of textile industry wastewater using bacterial and plant bioassays. *Toxicology Reports*, 6, 193–201. <https://doi.org/10.1016/j.toxrep.2019.02.002>
- Kłos, A., Ziembik, Z., Rajfur, M., Doñańczuk-Śródka, A., Bochenek, Z., Bjerke, J. W., et al. (2018). Using moss and lichens in biomonitoring of heavy-metal contamination of forest areas in southern and north-eastern Poland. *Science of the Total Environment*, 627, 438–449. <https://doi.org/10.1016/j.scitotenv.2018.01.211>
- Krika, F., Azzouz, N., & Ncibi, M. C. (2016). Adsorptive removal of cadmium from aqueous solution by cork biomass: Equilibrium, dynamic and thermodynamic studies. *Arabian Journal of Chemistry*, 9, S1077–S1083. <https://doi.org/10.1016/j.arabj.2011.12.013>
- Kumar, U. (2011). Thermodynamics of the adsorption of Cd(II) from aqueous solution on NCRH cylinder. *International Journal of Environmental Science and Development*, 334–336. <https://doi.org/10.7763/IJESD.2011.V2.147>
- Kumar, V., Parihar, R. D., Sharma, A., Bakshi, P., Singh Sidhu, G. P., Bali, A. S., et al. (2019). Global evaluation of heavy metal content in surface water bodies: A meta-analysis using heavy metal pollution indices and multivariate statistical analyses. *Chemosphere*, 236, 124364. <https://doi.org/10.1016/j.chemosphere.2019.124364>
- Long, J., Gao, X., Su, M., Li, H., Chen, D., & Zhou, S. (2018). Performance and mechanism of biosorption of nickel(II) from aqueous solution by non-living *Streptomyces roseorubens* SY. *Colloids and Surfaces A: Physicochemical and Engineering Aspects*, 548, 125–133. <https://doi.org/10.1016/j.colsurfa.2018.03.040>
- Mamindy-Pajany, Y., Sayen, S., & Guillon, E. (2013). Impact of sewage sludge spreading on nickel mobility in a calcareous soil: Adsorption–desorption through column experiments. *Environmental Science and Pollution Research*, 20(7), 4414–4423. <https://doi.org/10.1007/s11356-012-1357-3>
- Martinez, R. S., Sáenz, M. E., Alberdi, J. L., & Di Marzio, W. D. (2019). Comparative ecotoxicity of single and binary mixtures exposures of nickel and zinc on growth and biomarkers of *Lemna gibba*. *Ecotoxicology*, 28(6), 686–697. <https://doi.org/10.1007/s10646-019-02065-7>

- Min, K. J., Choi, S. Y., Jang, D., Lee, J., & Park, K. Y. (2019). Separation of metals from electroplating wastewater using electro dialysis. *Energy Sources, Part a: Recovery, Utilization, and Environmental Effects*, 41(20), 2471–2480. <https://doi.org/10.1080/15567036.2019.1568629>
- Mohammed, A. A., Najim, A. A., Al-Musawi, T. J., & Alwared, A. I. (2019). Adsorptive performance of a mixture of three nonliving algae classes for nickel remediation in synthesized wastewater. *Journal of Environmental Health Science and Engineering*, 17(2), 529–538. <https://doi.org/10.1007/s40201-019-00367-w>
- Mubarak, M. Z., & Lieberto, J. (2013). Precipitation of nickel hydroxide from simulated and atmospheric-leach solution of nickel laterite ore. *Procedia Earth and Planetary Science*. <https://doi.org/10.1016/j.proeps.2013.01.060>
- Nishikawa, E., da Silva, M. G. C., & Vieira, M. G. A. (2018). Cadmium biosorption by alginate extraction waste and process overview in life cycle assessment context. *Journal of Cleaner Production*, 178, 166–175. <https://doi.org/10.1016/j.jclepro.2018.01.025>
- Nnaji, C. C., Agim, A. E., Mama, C. N., Emenike, P. C., & Ogarekpe, N. M. (2021). Equilibrium and thermodynamic investigation of biosorption of nickel from water by activated carbon made from palm kernel chaff. *Scientific Reports*, 11(1), 7808. <https://doi.org/10.1038/s41598-021-86932-6>
- Noormohamadi, H. R., Fat'hi, M. R., Ghaedi, M., & Ghez-elbash, G. R. (2019). Potentiality of white-rot fungi in biosorption of nickel and cadmium: Modeling optimization and kinetics study. *Chemosphere*, 216, 124–130. <https://doi.org/10.1016/j.chemosphere.2018.10.113>
- Ohnuki, T., Sakamoto, F., Kozai, N., Sakai, T., Kamiya, T., Satoh, T., & Oikawa, M. (2003). Micro-pix study on sorption behaviors of cobalt by lichen biomass. *Nuclear Instruments and Methods in Physics Research Section b: Beam Interactions with Materials and Atoms*, 210, 407–411. [https://doi.org/10.1016/S0168-583X\(03\)01048-6](https://doi.org/10.1016/S0168-583X(03)01048-6)
- Peters, A., Schlekot, C. E., & Merrington, G. (2016). Does the scientific underpinning of regulatory tools to estimate bioavailability of nickel in freshwaters matter? The European-wide environmental quality standard for nickel. *Environmental Toxicology and Chemistry*, 35(10), 2397–2404. <https://doi.org/10.1002/etc.3510>
- Pipíška, M., Horník, M., Vrtoch, L., Augustín, J., & Lesný, J. (2008). Biosorption of Zn and Co ions by Evernia prunastri from single and binary metal solutions. *Chemistry and Ecology*, 24(3), 181–190. <https://doi.org/10.1080/02757540802069498>
- Priac, A., Badot, P.-M., & Crini, G. (2017). Treated wastewater phytotoxicity assessment using *Lactuca sativa*: Focus on germination and root elongation test parameters. *Comptes Rendus Biologies*, 340(3), 188–194. <https://doi.org/10.1016/j.crv.2017.01.002>
- Rangabhashiyam, S., Jayabalan, R., Asok Rajkumar, M., & Balasubramanian, P. (2019). Elimination of toxic heavy metals from aqueous systems using potential biosorbents: A review (pp. 291–311). https://doi.org/10.1007/978-981-13-1202-1_26
- Revellame, E. D., Fortela, D. L., Sharp, W., Hernandez, R., & Zappi, M. E. (2020). Adsorption kinetic modeling using pseudo-first order and pseudo-second order rate laws: A review. *Cleaner Engineering and Technology*, 1, 100032. <https://doi.org/10.1016/j.clet.2020.100032>
- Sarı, A., Tuzen, M., Uluözülü, Ö. D., & Soylak, M. (2007). Biosorption of Pb(II) and Ni(II) from aqueous solution by lichen (*Cladonia furcata*) biomass. *Biochemical Engineering Journal*, 37(2), 151–158. <https://doi.org/10.1016/j.bej.2007.04.007>
- Şenol, Z. M., Gül, Ü. D., Gurbanov, R., & Şimşek, S. (2021). Optimization the removal of lead ions by fungi: Explanation of the mycosorption mechanism. *Journal of Environmental Chemical Engineering*, 9(2), 104760. <https://doi.org/10.1016/j.jece.2020.104760>
- Şenol, Z. M., Gül, Ü. D., & Şimşek, S. (2019). Assessment of Pb²⁺ removal capacity of lichen (*Evernia prunastri*): Application of adsorption kinetic, isotherm models, and thermodynamics. *Environmental Science and Pollution Research*, 26(26), 27002–27013. <https://doi.org/10.1007/s11356-019-05848-x>
- Sharma, R., Jasrotia, T., Sharma, S., Sharma, M., Kumar, R. R., Vats, R., et al. (2021). Sustainable removal of Ni(II) from waste water by freshly isolated fungal strains. *Chemosphere*, 282, 130871. <https://doi.org/10.1016/j.chemosphere.2021.130871>
- Shen, Z., Zhang, Y., McMillan, O., Jin, F., & Al-Tabbaa, A. (2017). Characteristics and mechanisms of nickel adsorption on biochars produced from wheat straw pellets and rice husk. *Environmental Science and Pollution Research*, 24(14), 12809–12819. <https://doi.org/10.1007/s11356-017-8847-2>
- Singh, S. A., & Shukla, S. R. (2016). Adsorptive removal of cobalt ions on raw and alkali-treated lemon peels. *International Journal of Environmental Science and Technology*, 13(1), 165–178. <https://doi.org/10.1007/s13762-015-0801-6>
- Singh, S., & Shukla, S. R. (2017). Theoretical studies on adsorption of Ni(II) from aqueous solution using Citrus limetta peels. *Environmental Progress & Sustainable Energy*, 36(3), 864–872. <https://doi.org/10.1002/ep.12526>
- de Souza, R., Ambrosini, A., & Passaglia, L. M. P. (2015). Plant growth-promoting bacteria as inoculants in agricultural soils. *Genetics and Molecular Biology*, 38(4), 401–419. <https://doi.org/10.1590/S1415-475738420150053>
- Sudha, R., Srinivasan, K., & Premkumar, P. (2015). Removal of nickel(II) from aqueous solution using Citrus Limetioides peel and seed carbon. *Ecotoxicology and Environmental Safety*, 117, 115–123. <https://doi.org/10.1016/j.ecoenv.2015.03.025>
- Sundararaju, S., Manjula, A., Kumaravel, V., Muneeswaran, T., & Vennila, T. (2020). Biosorption of nickel ions using fungal biomass *Penicillium* sp. MRF1 for the treatment of nickel electroplating industrial effluent. *Biomass Conversion and Biorefinery*. <https://doi.org/10.1007/s13399-020-00679-0>
- Upreti, D. K., Divakar, P. K., & Nayaka, S. (2005). Commercial and ethnic use of lichens in India. *Economic Botany*, 59(3), 269–273. [https://doi.org/10.1663/0013-0001\(2005\)059\[0269:CAEUOL\]2.0.CO;2](https://doi.org/10.1663/0013-0001(2005)059[0269:CAEUOL]2.0.CO;2)
- USEPA. (1986). Health assessment document for nickel. National Center for Environmental Assessment, Office of Research and Development.

- Villen-Guzman, M., Cerrillo-Gonzalez, M. M., Paz-Garcia, J. M., Rodriguez-Maroto, J. M., & Arhoun, B. (2021). Valorization of lemon peel waste as biosorbent for the simultaneous removal of nickel and cadmium from industrial effluents. *Environmental Technology & Innovation*, 21, 101380. <https://doi.org/10.1016/j.eti.2021.101380>
- Wang, C., Li, T., Yu, G., & Deng, S. (2020). Removal of low concentrations of nickel ions in electroplating wastewater by combination of electrodialysis and electrodeposition. *Chemosphere*, 128208. <https://doi.org/10.1016/j.chemosphere.2020.128208>
- Wang, J., & Chen, C. (2009). Biosorbents for heavy metals removal and their future. *Biotechnology Advances*, 27(2), 195–226. <https://doi.org/10.1016/j.biotechadv.2008.11.002>
- Wang, Jiao, Liu, G., Li, T., & Zhou, C. (2015). Physicochemical studies toward the removal of Zn(Zn^{2+}) and Pb(Pb^{2+}) ions through adsorption on montmorillonite-supported zero-valent iron nanoparticles. *RSC Advances*, 5(38), 29859–29871. <https://doi.org/10.1039/C5RA02108A>
- Wu, D., Yu, X., Chu, S., Jacobs, D. F., Wei, X., Wang, C., et al. (2018). Alleviation of heavy metal phytotoxicity in sewage sludge by vermicomposting with additive urban plant litter. *Science of the Total Environment*, 633, 71–80. <https://doi.org/10.1016/j.scitotenv.2018.03.167>
- Wu, X., Huang, P., Dong, C., & Deng, X. (2021). Nickel bioaccumulation by a marine bacterium *Brevibacterium* sp. (X6) isolated from Shenzhen Bay, China. *Marine Pollution Bulletin*, 170, 112656. <https://doi.org/10.1016/j.marpolbul.2021.112656>
- Zinicovscaia, I., Yushin, N., Gundorina, S., Demčák, Š, Frontasyeva, M., & Kamanina, I. (2018). Biosorption of nickel from model solutions and electroplating industrial effluent using cyanobacterium *Arthrospira platensis*. *Desalination and Water Treatment*, 120, 158–165. <https://doi.org/10.5004/dwt.2018.22691>

Publisher's Note Springer Nature remains neutral with regard to jurisdictional claims in published maps and institutional affiliations.